

Layout Optimization of Multi-Material Continuum Structures with the Isolines Topology Design Method

Oswaldo M. Querin¹, Mariano Victoria², Concepción Díaz², and Pascual Martí²

¹School of Mechanical Engineering. University of Leeds

Leeds LS2 9JT, United Kingdom

e-mail: O.M.Querin@leeds.ac.uk

web: <http://www.mech-eng.leeds.ac.uk/menomq/>

²Departamento de Estructuras y Construcción. Universidad Politécnica de Cartagena

Campus Muralla del Mar. C/Doctor Fleming, s/n. 30202 Cartagena, España

e-mail: mariano.victoria@upct.es; conchi.diaz@upct.es; pascual.marti@upct.es

web: <http://www.upct.es/~deyc>

Keywords: Layout optimization, multi-material, ITD algorithm, isolines, continuum structures

Abstract:

A heterogeneous or multi-material object is one made from different materials which are distributed continuously or discontinuously and where its properties can be adjusted by controlling the material composition, microstructure and geometry of the object. The development of manufacturing technologies such as rapid prototyping can eliminate the high cost of tooling and can offer the possibility to make multi-materials structures. However the ability to design them is not a trivial task and requires the development or modifications of optimization algorithms to take into consideration the different aspects of these problems. This article presents an enhancement to the ITD

algorithm which allows it to obtain multi-material designs. Four examples of the topology design of 2D continuum structures are presented to demonstrate that the ITD algorithm is an efficient and reliable method to carry out the layout optimization of multi-material continuum structures.

1 INTRODUCTION

In the past, the intuition and experience of designers played a key role in structural design. The last few decades have seen remarkable advances made in topology optimization, which provides conceptual layouts for a given design space and specified boundary conditions. There are a lot of methods, but these can be divided into one of two types: 1) Those with a mathematical basis (Homogenization and Solid Isotropic Microstructure with Penalization (SIMP), Level set method (LSM)); and 2) those based on heuristics (Soft Kill (SK), Hard Kill (HK), Evolutionary Structural Optimization (ESO), Additive ESO (AESO), Bidirectional ESO (BESO), Reverse Adaptivity (RA), etc). The aim of these methods is to support the intuition and the experience of a designer. In addition, most of these methods are focused on the optimization of traditional structures consisting of one material.

A heterogeneous or multi-material object is referred to as a solid object made of different materials distributed continuously or discontinuously and its properties can be adjusted by controlling the material composition, microstructure and the geometry of the object (Jadayil 2011).

In many applications, the object should have certain characteristics to be able to develop its function as: Heat resistance, anti-oxidation properties, high yield stress or ultimate tensile strength, etc. Such properties may not be obtained by using single or homogeneous material.

The development of new manufacturing technologies such as rapid prototyping (Bhashyam et al. 2000) or solid free form fabrication (Beaman et al. 1997, Jakubenas et al. 1998), and the use of new materials like composites (Blasques and Stolpe 2012) requires new optimization techniques. These emerging manufacturing technologies eliminate the high cost of tooling and design changes or material substitution and offer the possibility to achieve multi-materials structures. However, this makes it much more difficult to design objects just by intuition. Hence, new optimization algorithms are needed to provide designs which take into account all the different aspects of such a problem (König and Fadel 1999).

Objects with varying properties across spatial domain are commonly used in aerospace, biomedical, civil, geophysical and nano-scale structures. In these applications, the performance objectives are reached due to the capability of varying material properties globally and locally across the design domain.

Thomsen (1992) maximized the integral stiffness of a structures composed of one or two isotropic materials using the homogenization technique. Material was modelled by a second rank composite using the concentration and orientation of the composite as design variables.

Sigmund and Torquato (1997) presented a topology optimization method to design material microstructures with extreme thermoelastic properties. The method consists in finding the distribution of material phases that optimizes the isotropic thermal expansion (i.e. the sum of the thermal strain coefficients in the horizontal and the vertical directions) subjected to constraints, such as elastic symmetry or volume fractions of the constituent phases, within a periodic base cell. The effective properties of the material structures were found using the homogenization method.

Sigmund (2001) demonstrated that topology optimization can be used as a systematic tool for the design of two-material MicroElectroMechanical Systems (MEMS). The topology optimization method was extended to multiple materials by introducing two design variables per element. One variable determines whether there is material in the element or not and the other variable determines the type of material. The interpolation of the material properties was made using a hybrid scheme, where the power-law approach was used to interpolate between void and material and a weighted average of the upper and lower Hashin-Shtrikman bounds (Hashin and Shtrikman 1963) were used to interpolate between the material types.

Yin and Ananthasuresh (2001) proposed a new material interpolation model, called the peak function model. By using the peak function and the optimality criteria method, they synthesized compliant mechanisms with multiple materials with and without the material resource constraint.

Saxena (2002) discussed the discrete density parameterization with multiple-material handling in topology optimization of compliant mechanisms. Genetic algorithm was the search algorithm using fitness function values to guide a probabilistic search towards a possible global optimum.

Yulin and Xiaoming (2004) applied LSM to a general optimization problem with multi-materials and multi-constraints, such as a stiff structure design, a compliant mechanism design or a material design by using the different material representation models.

Wang and Wang (2004) addressed the problem of structural shape and topology optimization in a multi-material domain. The LSM was used as an alternative approach to the homogenization method of rule of mixtures for multi-material modelling.

Jung and Gea (2006) proposed a new multi-material model to formulate the topology optimization problem for energy absorption. A three-phase material model for topology optimization was derived to accommodate two conflicting design objectives: 1) Minimize the mean compliance; and 2) Maximize the strain energy for energy absorption.

Zhou and Wang (2007) introduced a phase field model for the optimization of multi-material structural topology based a modified Cahn-Hilliard theory. They treated the problem of minimizing the mean compliance of a multi-material structure as a thermodynamic system with mass concentration as phase field variable.

Huang and Xie (2009) developed a new and generalized BESO method with a penalization parameter for continuum structures with one or multiple materials utilizing a material interpolation scheme.

Gao et al. (2010) investigated the topology optimization problem of multiple materials with mass constraint. Two types of material interpolation schemes named Generalized Solid Isotropic Material with Penalization (GSIMP) and Uniform Interpolation Model (UIM) were considered.

Ramani (2010) presented an algorithm which uses material as a discrete variable in multi-material topology optimization and thus provides an alternative to traditional methods using material interpolation and level-set approaches. The algorithm computes pseudo-sensitivities of the objective and constraint functions to discrete material changes. These are used to rank elements, based on which fraction of the elements are selected for material ID modification during the optimization iteration. Subsequently, a heuristic approach to handle strength constraints based on the material failure criteria in multi-material was also introduced by Ramani (2011).

Luo et al. (2012) presented a topology optimization methodology considering non-probabilistic reliability for the design of two-material continuum structures whose objective was to distribute a given amount of two candidate materials into the design domain for acquiring the maximum stiffness while satisfying the reliability requirements.

Blasques and Stolpe (2012) introduced a novel approach for the simultaneous optimization of the topology and laminate properties in the structural design of laminated composite beam cross sections. The optimization is based on a multi-material topology optimization model in which the design variables represent the amount of the given materials in the cross section. Existing material interpolation, penalization, and filtering schemes were extended to accommodate any number of anisotropic materials.

This article presents the extension of the Isolines Topology Design (ITD) algorithm (Victoria et al. 2009) to the design multi-material structures. The method of determining the isolines is given, together with four examples to show the effectiveness of the algorithm. The results show the usefulness of ITD to provide quality solutions with very detailed shapes, without the need to interpret the design.

2 TOPOLOGY DESIGN WITH MULTI-MATERIALS TECHNIQUES

Currently, the most used techniques for topology design of continuum structures using heterogeneous or multiple materials are: 1) Material interpolation schemes (Yin and Ananthasuresh 2001, Huang and Xie 2009, Gao et al. 2010, Luo et al. 2012, Blasques and Stolpe 2012,); 2) Level-set models (Yulin and Xiaoming 2004, Wang and Wang 2004, Zhuang et al. 2007); and 3) Phase-field schemes (Bourdin and Chambolle 2000, Jung and Gea 2006, Zhou and Wang 2007).

In material interpolation schemes, the overall mechanical properties of a multi-material object are commonly obtained using a “rule of mixture”. For the three-phase material design with two solid materials and void, the following power-law interpolation scheme is commonly used to obtain an artificial elasticity modulus (E) as

$$E(\rho_1, \rho_2) = \rho_1^p (\rho_2^p E_1 + (1 - \rho_2^p) E_2) \quad (1)$$

where E_1 and E_2 are the moduli of the solid material phases, $\rho_1 \in [0,1]$ and $\rho_2 \in [0,1]$ are the design density variables, and $p > 1$ is the penalization parameter for the intermediate densities. Others interpolation schemes are also in use, such as the Halpin-Tsai composite model (Suresh and Mortensen 1988), Voigt-Reuss (Swan and Kosaka 1997) and Hashin-Shtrikman (Sigmund 2001).

To model more than two phases using the LSM one may consider using multi-level set functions to partition the whole material domain of the structure with each level set representing a distinct material phase (Zhao et al. 1998, Tsai et al. 2001).

Wang and Wang (2004) proposed a new multi-material model based on multi-phase level-set scheme developed by Vese and Chan (2002).

They considered m level-set functions

$$\phi_i(x): D \rightarrow R(i = 1, \dots, m) \quad (2)$$

where D is the design domain.

Instead of using each level set to represent each distinct material phase as in the partitioning level-set scheme, they allowed the interior regions of the zero-level sets of these functions $\Omega_i = \{x: \phi_i(x) > 0\}$ to overlap. They then defined the union of these zero-level sets $\Gamma_i = \{x: \phi_i(x) = 0\}$ to represent the boundaries of the multi-phase

material regions and denoted the disjointed but connected regions formed by these boundaries $\Gamma = \bigcup_{i=1}^n (\Gamma_i)$ by w_k , Eq. (3).

$$D = \bigcup_{k=1}^n w_k \quad \text{and} \quad w_k \cap w_l = \emptyset, k \neq l \quad (3)$$

where n is the number of materials.

To illustrate this, an example of four material phases ($n = 4$) and two level-set functions ($m = 2$) is depicted in Fig. 1.

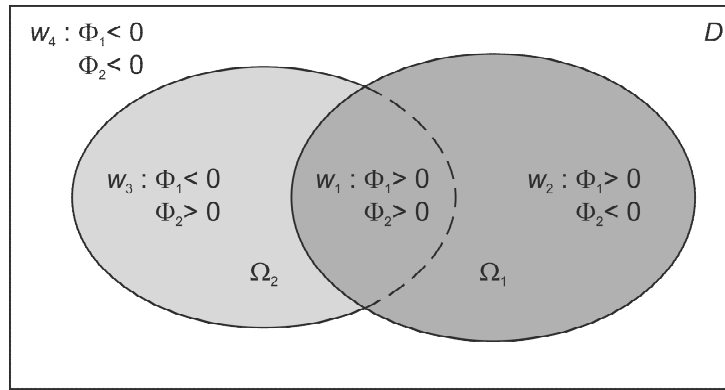


Fig. 1. Four material phases (w_1, w_2, w_3, w_4) are represented by two-level set functions (ϕ_1, ϕ_2).

Phase field schemes have for a long time been used as a practicable scheme for interpreting a wide variety of material phenomena like diffusion and solidification. The material may be solid or liquid of two or more phases. The usual problem is to characterize the stability of such a system and to describe the interface between the phases while the system undergoes a physical process to reach its stability (Zhou and Wang 2007). In spite of the fact that there is a clear relationship between the problem of topology optimization of a solid multi-material structure and a phase transition system of material phases, the use of these schemes has not yet become popular. Hence, there are few approaches in the literature Wang and Zhou (2004), Burger and Stainko (2006), and Takezawa et al. (2010).

3 FIXED GRID FINITE ELEMENT ANALYSIS

The Fixed Grid (FG) method was first introduced by Garcia and Steven (1999) as a tool for numerical estimation of two-dimensional (2D) elasticity problems, and was extended to three-dimensional (3D) structures like Garcia et al. (2004, 2005), etc. The benefits of using FG-Finite Element Analysis (FEA) over conventional FEA in this work are that: 1) FG does not need a fitted mesh to discretize the analysis domain; 2) The boundary of the design is disassociated from the mesh (Garcia and Steven 1999); 3) Designs using FG-FEA do not contain checkerboard patterns, making the design more reliable for manufacture (Maan et al. 2007); and 4) Solution time is significantly reduced (Garcia and Steven 2000). In FG-FEA, the elements are in a fixed position and have the real design superimposed on them. This means that there are elements which lie Inside (I), Outside (O), or on the Boundary (B) of the design.

The elemental stiffness matrix (\mathbf{K}^e) is given by Eq. (4).

$$\mathbf{K}^e = \begin{cases} \mathbf{K}_I & \text{if } \xi^e = 1 \\ \mathbf{K}_O & \text{if } \xi^e = 0 \\ \mathbf{K}_B = \mathbf{K}_I \xi^e + \mathbf{K}_O (1 - \xi^e) & \text{if } 0 < \xi^e < 1 \end{cases} \quad (4)$$

where ξ^e is the design fraction inside the element, \mathbf{K}_I is the element stiffness matrix for an element inside, \mathbf{K}_O is the element stiffness matrix for an element outside, and \mathbf{K}_B for an element boundary. Normally $\mathbf{K}_O = 10^{-6} \times \mathbf{K}_I$.

In this work, the criterion value in each element (σ^e) is calculated using Eq. (5)

$$\sigma^e = \frac{\sum_{k=1}^{n_G} w_k \sigma_k^e}{\sum_{k=1}^{n_G} w_k} \quad (5)$$

where n_G is the number of the Gauss points in the element, and w is the weighting factor for each Gauss point.

The criterion value at the i node of an element σ_i^n is determined by Eq. (6)

$$\sigma_i^n = \sum_{e=1}^N \sigma_{n_i}^e / N \quad (6)$$

where i is the i^{th} node number of an element, $\sigma_{n_i}^e$ is the nodal criterion value at node i for each element surrounding that node, and N is the number of elements connected to that node. The nodal value is determined from the criterion values at each Gauss point extrapolated to the nodes using the shape functions of the element.

4 MULTI-MATERIAL DESIGN WITH ISOLINES

The use of isolines/isosurfaces in 2D/3D respectively to obtain the optimum design of structures has been used in several studies (Woon et al. 2003, Cui et al. 2003, Koguchi and Kikuchi 2006). The ITD is an iterative algorithm which redistributes (adds and removes) material inside of a design domain until it reaches a desired volume fraction. The redistribution process consists of the following four steps: 1) Obtain the design criterion distribution within the design domain; 2) Determine the Minimum Criterion Level (MCL), where its intersection with the design criterion distribution produces the new structural boundary, shown for a 2D continuum in Fig. 2; 3) Remove all regions from the design domain where the criterion distribution is lower than the MCL; and 4) This design modification requires the re-evaluation of the remaining structure in order to recalculate the design criterion distribution.

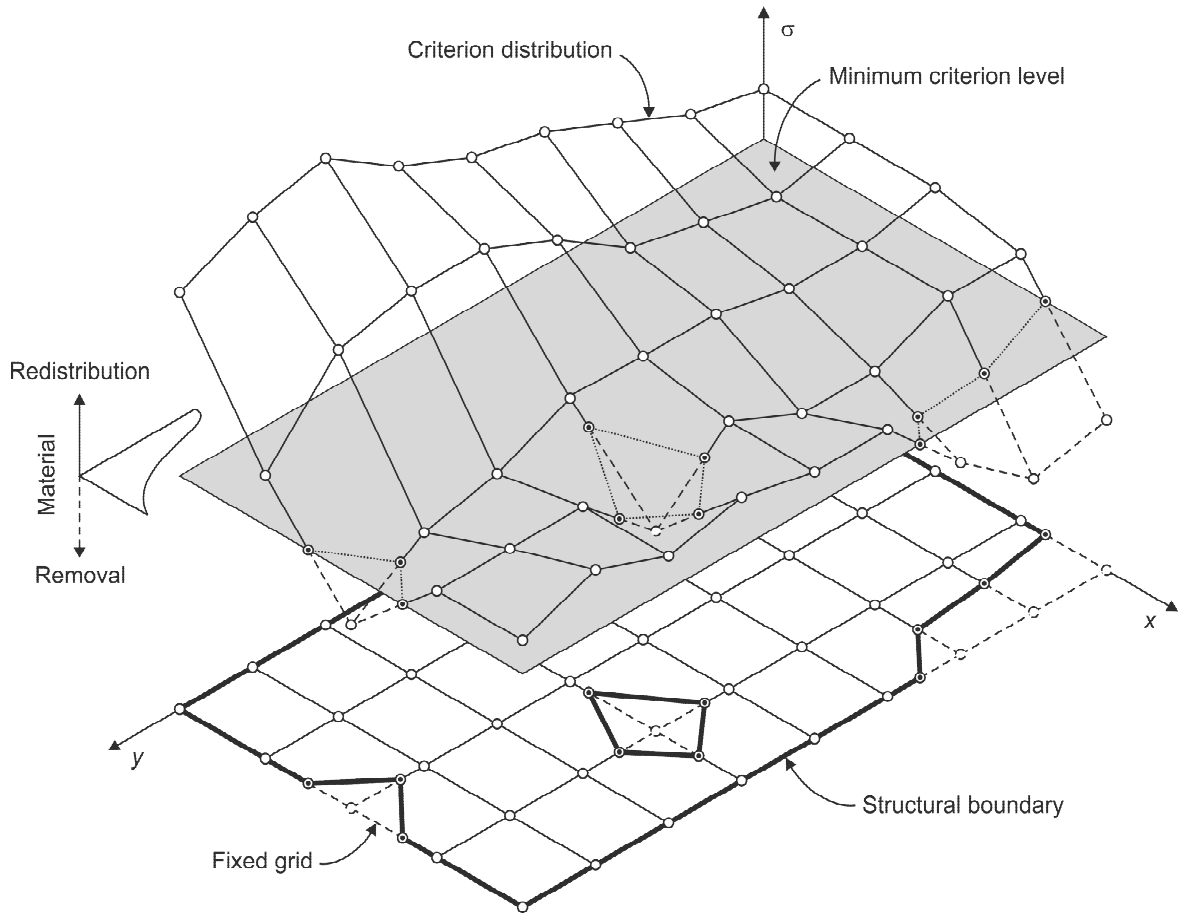


Fig. 2. Structural boundary is defined by the intersection of the MCL with the criterion distribution.

The MCL is calculated in each iteration and depends on both the distribution of the design criterion and the volume of the design domain in that iteration given by Eq. (7)

$$V_i = V_0 \left(\frac{n_i - i}{n_i} \right) + V_f \left(\frac{i}{n_i} \right) \quad (7)$$

where V_i is the design volume in the i^{th} iteration, n_i is the total number of iterations, V_0 is the initial volume, and V_f is the final volume of the optimized structure.

Once the criterion has been calculated for each element in the design domain, these are arranged in decreasing order of criterion value. An element by element volume summation of the ordered list is carried out until a volume is reached which is as close as possible to the target volume given by Eq. (7), where the error level

between the summed and target volume depends on the size of the elements. The criterion value of the next element in the ordered list is then used as the value for the MCL.

4.1 Optimization problem

The optimization problem (Eq. 8 and 9) consisted of minimizing the difference between the structure volume and a target volume subject to: 1) Structural equilibrium; and 2) An inequality condition which must be satisfied by all the nodes of the structure.

Minimize:

$$V_0 - V_f \quad (8)$$

Subject to:

$$\begin{aligned} \mathbf{K}\mathbf{u} - \mathbf{P} &= 0 \\ \sigma_{\text{MCL}} - \sigma_i &\leq 0 \end{aligned} \quad (9)$$

where:

- K** is the structure stiffness matrix
- u** is structure displacement vector
- P** is the nodal load vector
- σ_{MCL} is the value of the minimum criterion level
- i i th node which lies inside or on the boundary of the structure
- σ_i is the value of the design criterion in the i th node

4.2 Criterion selection

The design criterion (σ^e) used in this work was the von Mises stress (σ_{vM}), which for a two-dimensional continuum domain is calculated using Eq. (10).

$$\sigma_{\text{vM}} = \sqrt{\sigma_x^2 + \sigma_y^2 - \sigma_x \sigma_y + 3\tau_{xy}^2} \quad (10)$$

where σ_x , σ_y and τ_{xy} are the axial and shear stresses, respectively.

4.3 Solid phase distribution to produce multi-material design

The idea to obtain multi-material stiff designs using the ITD algorithm is straightforward; the high values of the design criterion must be supported by the solid phases with the highest stiffness and vice versa. This is achieved by the 5 steps given below:

1. Determine the volume (V_i) of the design domain in the current i^{th} iteration using Eq. (7) and obtain the MCL value (σ_{MCL}) associated with V_i .
2. Arrange the j -material types ($j=1, \dots, n$) in decreasing order of stiffness value using the Young's moduli. The greatest value of the Young's modulus is termed E_1 and the smallest value is termed E_n .
3. Calculate the volume for every solid phase (V_j) in the current i^{th} iteration, using Eq. (11)

$$\begin{aligned} V_j &= \beta_j \times V_i \\ \sum_{j=1}^n \beta_j &= 1 \end{aligned} \quad (11)$$

where β_j is the volume control weighting factor. Its value is initially proposed by the designer.

4. Calculate the MCL for each solid phase $\sigma_{\text{MCL},j}$ associated with $V_{i,j}$ by Eq. (12), see Fig. 3.

$$V_{i,j} = \sum_{j=1}^j V_j \quad (12)$$

- Use the design fraction inside the element (ξ^e) and the minimum criterion level for each phase ($\sigma_{MCL,j}$) to determine material properties for every element (E^e) by Eq. (13), see Fig. 3.

$$E^e = \begin{cases} E_0 & \text{if } \xi^e = 0 \\ E_j & \text{otherwise} \end{cases}$$

$$E_0 = 10^{-6} \times E_n$$

$$E_j = \begin{cases} E_1 & \text{if } \sigma^e > \sigma_{MCL,1} \\ E_2 & \text{if } \sigma_{MCL,2} \leq \sigma^e < \sigma_{MCL,1} \\ \vdots & \vdots \\ E_n & \text{if } \sigma_{MCL,n} \leq \sigma^e < \sigma_{MCL,n-1} \end{cases} \quad (13)$$

where:

- E_0 is the Young's modulus for void phase
- E_n is the Young's modulus for n -material (i.e. the weakest material)
- E_j is the Young's modulus of the j th material
- σ^e is the elemental value of the criterion

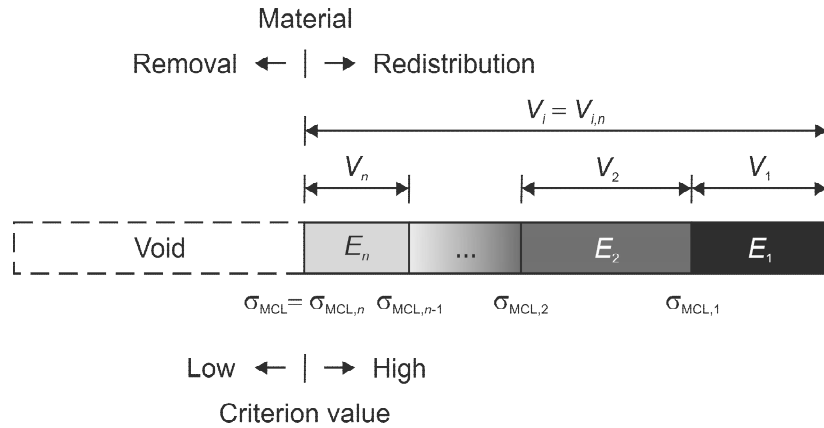


Fig. 3. Schematic diagram for distribution of j -materials.

4.4 Minimum criterion level extraction

The procedure to generate the structural boundary depends on the determination of the MCL isoline. In order to determine the line segments that produce the profile of

the boundary, the contouring subroutine called Marching Triangles (MT) algorithm (Hinton and Illingworth 1997) was implemented, since there are not ambiguities and the isolines constructed are smooth.

The MT algorithm uses a divide-and-conquer approach, treating each finite element independently as a triangular cell. In the case where the element shape is quadrilateral, the element is divided into four triangular cells by introducing a point at the centroid of the element. The criterion value of the central point is obtained by calculating the average values from the four nodes of the original element. The basic assumption of this algorithm is that a contour can only pass through a triangular cell in a limited number of ways. This algorithm requires the value of the MCL together with the value of the criterion at each corner of the cell, and consists of two steps: 1) Identify from Fig. 4 the topological state of each cell; and 2) Determine the shape of the contour of the MCL isoline through each cell. The interaction of an isoline through a triangular cell can have a maximum of four different topological states, Fig. 4. The value (1) at a corner means that its criterion value is greater than the MCL whereas a value of (0) at a corner means that its criterion value is less than the MCL. When the corner in an edge of a cell has different values (0 and 1 or vice versa) it indicates that the MCL isoline intersects that edge, which is the case for topological states shown in Fig. 4b and 4c. To find that intersection point, linear interpolation can be used. The shape of the MCL isoline through the cell is then obtained by connecting these intersecting points between the opposite edges as shown in Fig. 4b and 4c.

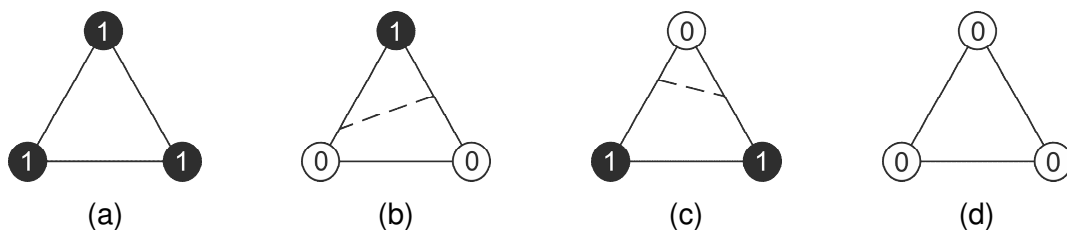


Fig. 4. Look-up table for the MT algorithm showing the four different topological states.

4.5 Structural boundary stabilization

When the MCL is modified, the structural boundary changes and this affects the criterion distribution. Therefore, before the next iteration is started, an iterative process of reanalysis and material redistribution is carried out until the change in the domain volume between successive boundary adjustments is less than a minimum volume change limit (ΔV), given by Eq. (14). Typical values of the minimum volume change limit are around $\Delta V(\%) = 1\%$.

$$\Delta V(\%) = \left(\frac{V_i}{V_{i-1}} - 1 \right) \times 100 \quad (14)$$

5 THE ITD ALGORITHM FOR MULTI-MATERIAL DESIGNS

The modified ITD algorithm to carry out the layout optimization of multi-material designs consists of the following eleven steps, a schematic representation of which is given in Fig. 5.

1. Define the structure: design and non-design domains, total number of materials (n), material properties for every material (E_j), loads and supports.
2. Specify the finite element mesh characteristics.
3. Specify the ITD parameters: design criterion (σ), volume control weighting factor (β_j), final design volume (V_f), total number of iterations (n_i), and minimum volume change limit ($\Delta V(\%)$).
4. Carry out a FG-FEA.
5. Determine the target volume for every material type ($V_{i,j}$).
6. Calculate the MCL value for every material type ($\sigma_{MCL,j}$).

7. Extract the boundary of the structure and distribute the different materials.
8. If the percentage volume change is greater than the minimum volume change limit ($\Delta V(\%)$), go to step 9, otherwise go to step 10.
9. Carry out a FG-FEA of the design domain and go to step 7.
10. If the total number of iterations (n_i) has been reached, go to step 11, otherwise update the design volume, increment the iteration number (i) by 1 and go to step 4.
11. Stop the design process.

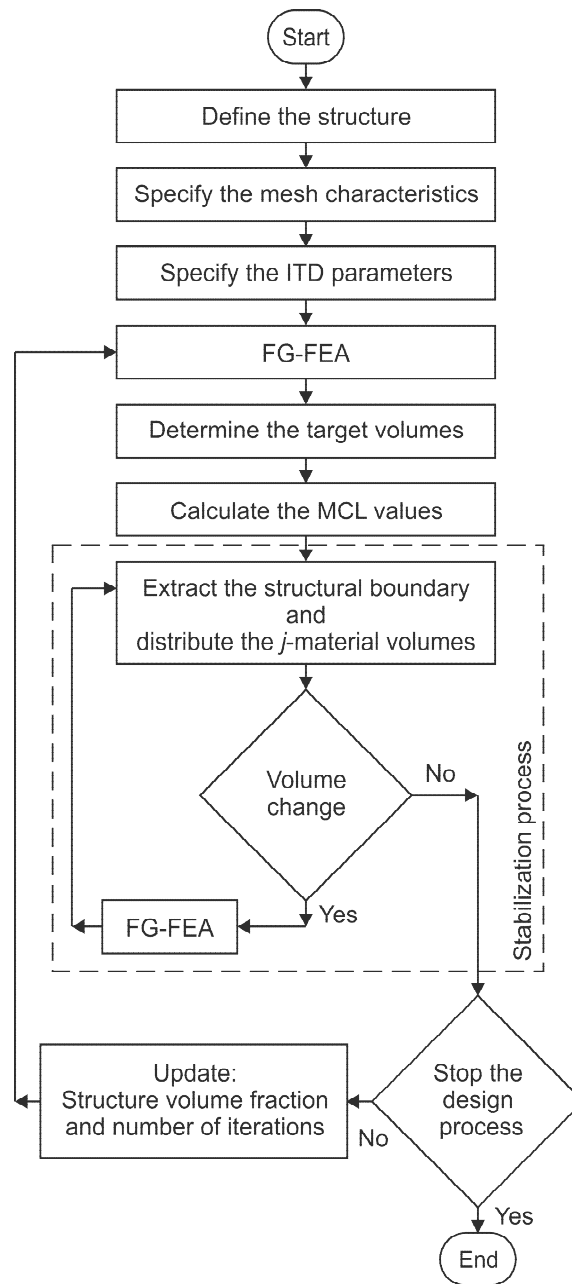


Fig. 5. Flow chart of the ITD algorithm applied to the multi-material topology design.

6 EXAMPLES

To illustrate the ITD algorithm, four structures were studied and are presented here:
 1) A short cantilever loaded at the lower free end; 2) A short cantilever loaded at the middle free end; 3) A beam with a roller support; 4) A metallic insert. The FE used for the examples is the four-node plane stress quadrilateral element with four Gauss

integration points. Table 1 shows the colour legend used to represent the resulting multi-material designs.

Table 1. Colour legend for multi-material designs

Total number of material	Material code number			Void
	1	2	3	
2	Black	Grey	-	White
3	Black	Grey	Light grey	White

6.1 Short cantilever loaded at the lower free end

The first example is a short cantilever as is showed in Fig. 6. The design domain is a rectangular area of 16×10 m and the thickness is 0.05 m. The mesh used for the discretization of the design domain has 144×90 elements, fully clamped along the left edge. A vertical load of 200 kN is applied at the lower free end in the downward direction. Two materials were used with the Young's moduli of $E_1 = 200$ GPa and $E_2 = 100$ GPa and the same Poisson's ratio $\nu = 0.3$. The ITD parameters for this example were the total number of iterations $n_i = 100$; final volume fraction $V_f/V_0 = 0.1$ and the minimum volume change $\Delta V(\%) = 1\%$. To examine the effect of the volume control weighting factor β_1 on the final design, eight cases were investigated: $\beta_1 = 0.2; 0.3; 0.4; 0.5; 0.6; 0.66; 0.7; \text{ and } 0.8$.

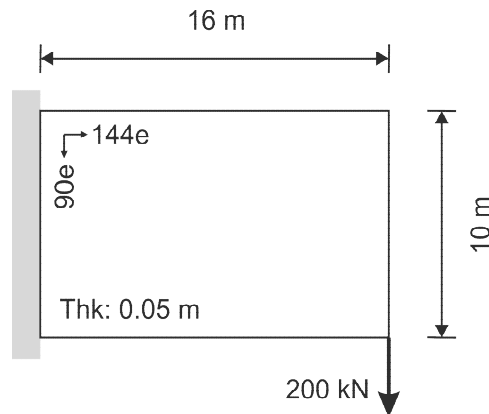
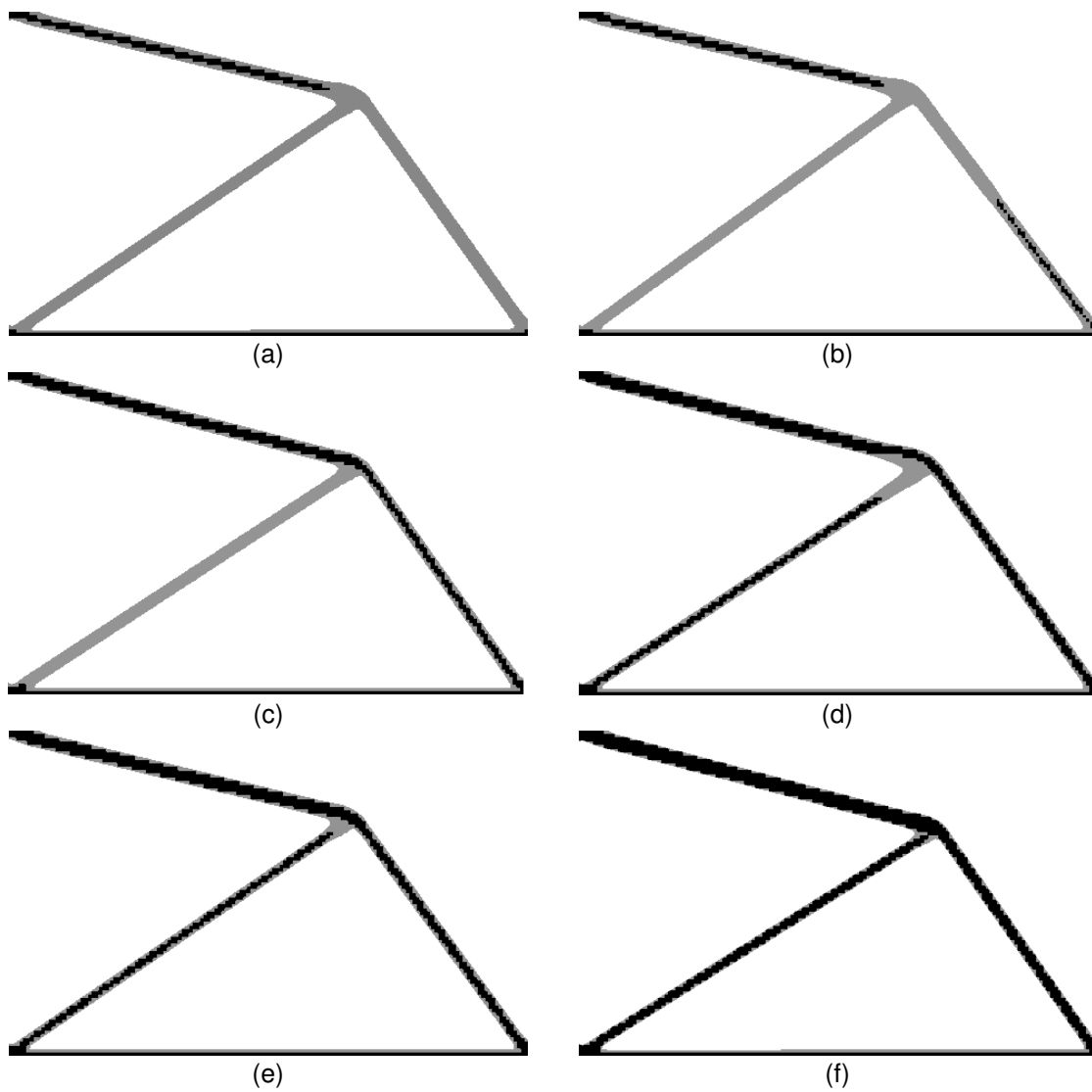


Fig. 6. Design domain for the short cantilever loaded at the lower free end.

Fig. 7 shows the resulting final topologies for each β_1 value. This has shown that the optimal topologies (which suggest a four-bar truss design) are not affected significantly by volume control weighting factor, except $\beta_1 = 0.8$ (which suggests a six-bar truss design). The resulting multi-material design depicted in Fig. 7f is in good agreement with that obtained by Luo et al. (2012).



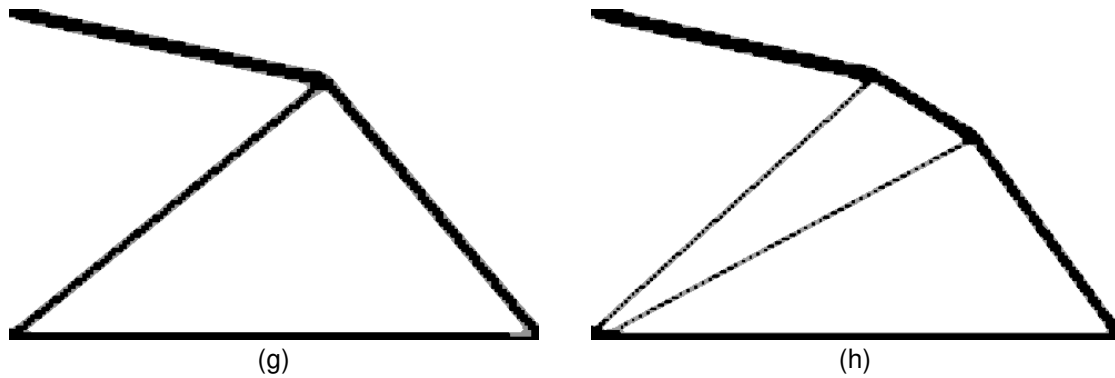


Fig. 7. Final designs for two-material scheme. Effect of different β_1 on final design: (a) 0.2 (b) 0.3 (c) 0.4 (d) 0.5; (e) 0.6; (f) 0.66; (g) 0.7; (h) 0.8.

6.2 Short cantilever loaded at the middle free end

The design domain, support conditions, and mesh characteristics used in this example are the same with the first example. A vertical load of 200 kN is applied at the middle free end in the downward direction (Fig. 8). The ITD parameters were the total number of iterations $n_i = 100$, final volume fraction $V_f/V_0 = 0.1$, the minimum volume change $\Delta V(\%) = 1\%$ and the volume control weighting factor $\beta_1 = 0.5$. To examine the effect of the material properties on the final design, four cases were investigated $E_1 = 200 \text{ GPa}$ with $E_2 = 150, 100, 50$ and 20 GPa . The same Poisson's ratio of 0.3 was used.

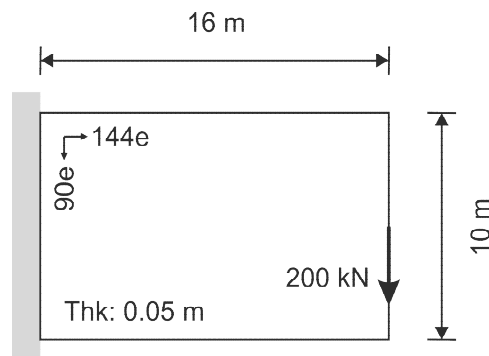


Fig. 8. Design domain for the short cantilever loaded at the middle free end.

The resulting multi-material designs are depicted in Fig. 9. The resulting topologies are not sensitive to the Young's modulus value (E_2), although it can be observed considerable differences between the final shape designs. The obtained designs are in good agreement with those obtained by Wang and Wang (2005).

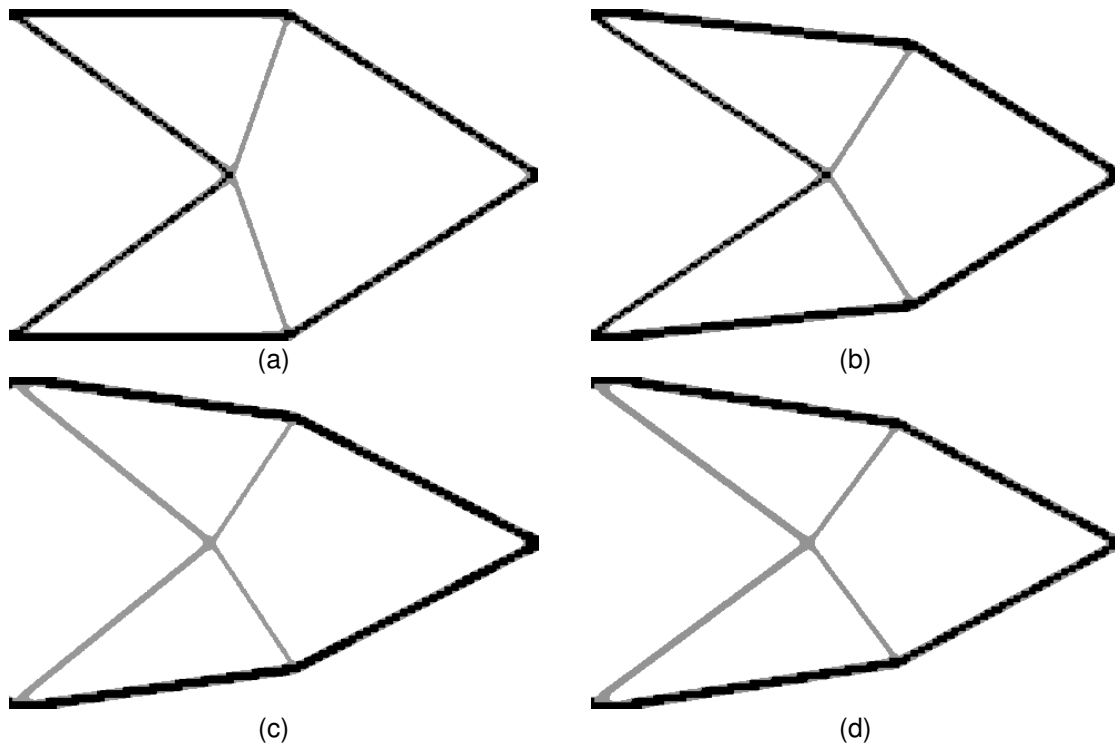


Fig. 9. Final designs for two-material scheme. Effect of different Young's modulus E_2 values on final design: (a) 150 GPa; (b) 100 GPa; (c) 50 GPa; (d) 20 GPa.

6.3 Beam with a roller support

The size of the beam is 24 m long by 4 m high with a thickness of 0.05 m (Fig. 10). It has a fixed support in the bottom left-hand corner and a roller support on the bottom-right corner. A vertical load of 200 kN in downward direction is applied at the centre of the bottom edge. The mesh used has 360×60 elements. The ITD parameters used were the total number of iterations $n_i = 100$, final volume fraction $V_f/V_0 = 0.1$, and the minimum volume change $\Delta V(\%) = 1\%$. In this example, the influence of the material number was investigated for two cases: 1) A two-material scheme, with $E_1 = 1$ GPa

and $E_2 = 0.1 \text{ GPa}$, and a volume control weighting factor $\beta_1 = 0.375$; and 2) A three-material scheme, with $E_1 = 1 \text{ GPa}$; $E_2 = 0.5 \text{ GPa}$ and $E_3 = 0.1 \text{ GPa}$. The second case was studied for four different volume control weighting factors $\beta_1 / \beta_2 / \beta_3$: (a) 0.2/0.4/0.4; (b) 0.2/0.6/0.2; (c) 0.4/0.2/0.4 and (d) 0.6/0.2/0.2. The same Poisson's ratio of 0.3 was used in both cases.

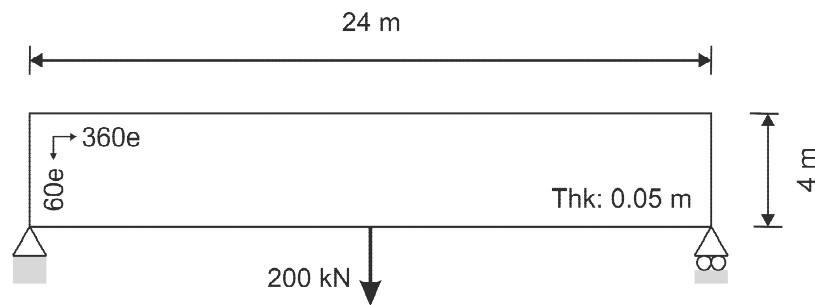


Fig. 10. Design domain for the beam with a roller support.

The final design for two-material scheme is shown in Fig. 11. The resulting design depicts a sandwich structure with a stiff skin manufactured using material No.1 and a soft truss core made in material No. 2. Note that, the resulting topology shows great agreement with the work of Huang and Xie (2009).

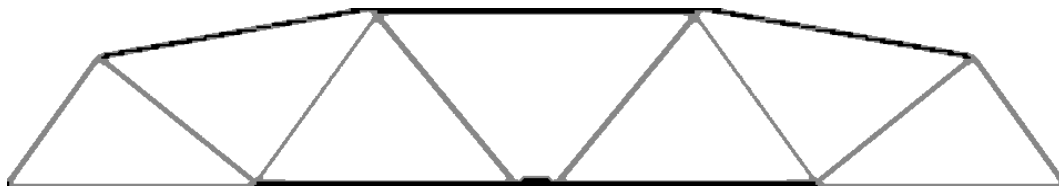
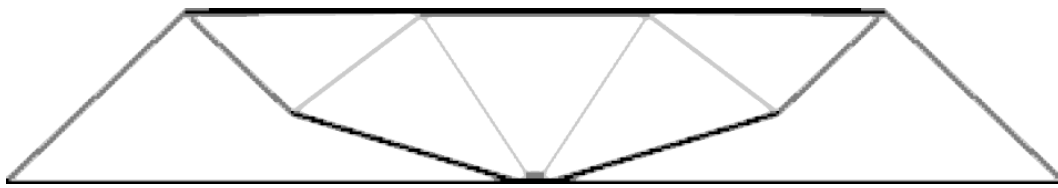
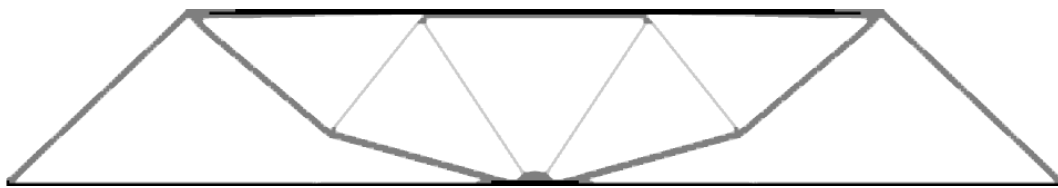


Fig. 11. Final design for two-material scheme.

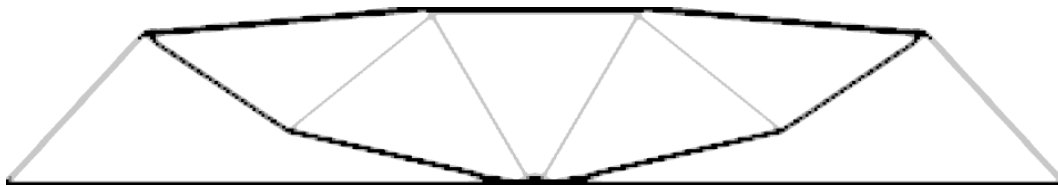
As for the two-material case, the optimal designs obtained using the three-material scheme are similar to the sandwich structure of (Fig. 11). The topology and shape of the resulting designs are significantly sensitive to weighting factor combinations. Note that, when material number increases the use of advanced technologies to manufacture these designs plays a crucial role.



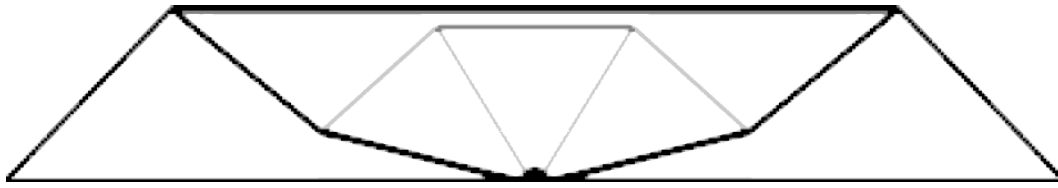
(a)



(b)



(c)



(d)

Fig. 12. Final designs for three-material scheme. Effect of different weighting factor combinations $\beta_1 / \beta_2 / \beta_3$ on design: (a) 0.2/0.4/0.4; (b) 0.2/0.6/0.2; (c) 0.4/0.2/0.4; (d) 0.6/0.2/0.2

6.4 Metallic insert

A theoretical and experimental investigation by Nilsson (1989) on increasing the bearing strength of composite bolted joints showed that by bonding a 2 mm circular metallic insert in the hole, the compressive stresses at the hole boundary were reduced by 50% and the failure load was increased by up to 55%. The purpose of this example is to optimize the shape of the insert by an optimized material distribution using ITD algorithm.

The geometric dimensions together with the loading and support conditions are shown in Fig. 13a. Due to the symmetry conditions, the analysis was made using only top-half of the domain using a regular rectangle mesh (Rispler and Steven 1995). The mesh features were 93,956 elements, 94,605 nodes, 189,210 degrees of freedoms. To ensure that the internal diameter remains unchanged in order to allow usage of currently available fasteners the nearest region around the hole boundary is defined as non-design domain. The bolt hole loading was represented by a linear pressure distribution (Fig.13b). The ITD parameters for this example were the total number of iterations $n_i = 5$, final volume fraction $V_f/V_0 = 1$ and the minimum volume change $\Delta V(\%) = 1\%$. The material properties used for the material No. 1 (aluminium) were

$E_1 = 71 \text{ GPa}$ and $\nu_1 = 0.3$, and for the material No. 2 (composite) were $E_2 = 52.2 \text{ GPa}$ and $\nu_2 = 0.33$. Six area ratios of material No.1 (A_1) with respect to hole area (A_H) were investigated: $A_1/A_H = 0.25:1, 0.5:1, 0.75:1, 1:1, 2:1$ and $3:1$.

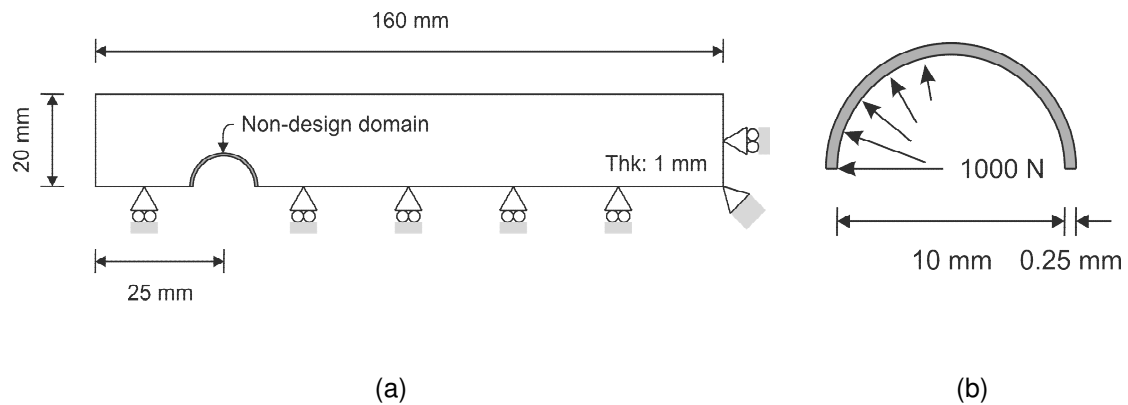


Fig. 13. Design domain for the metallic insert: (a) General dimensions and support conditions; (b) Detailed view of the loading.

The resulting solutions are shown in Fig.14. In order to achieve a clearer designs the black colour represents the aluminium material, the grey colour stands for the non-design domain, and the composite material was not depicted. The obtained shape of the inserts agrees with the solutions obtained by Rispler and Steven 1995.



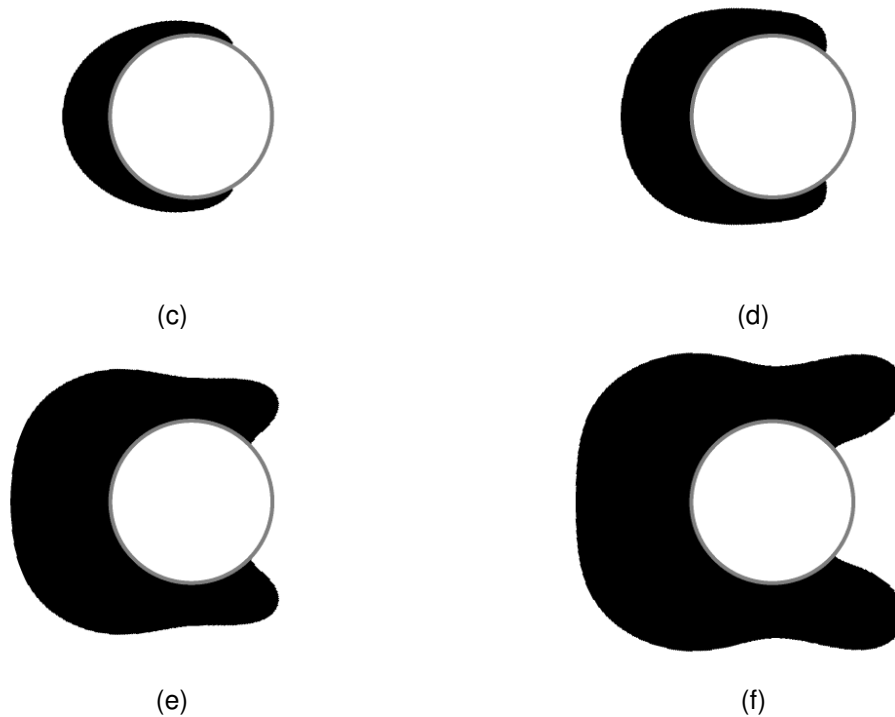


Fig. 14. Final insert (full detail view) for different area ratios of material No. 1 (in black) with respect to hole area (A_1/A_H): (a) 0.25:1, (b) 0.5:1, (c) 0.75:1, (d) 1:1, (e) 2:1 and (f) 3:1. The non-design domain is shown in grey.

7 CONCLUSIONS

This article presents an enhancement to the ITD algorithm which allows it to obtain multi-material designs. The ITD is an iterative process, where the generation of new contours allow the removal and redistribution of material. It allows for important topology changes during the design process. The placement of the multiple materials into the design is determined by the distribution of the design criterion (i.e. von Mises stress) following the concept that the material of highest stiffness must support the regions of the design with the highest design criterion.

Four examples of topology design of 2D continuum structures are presented to demonstrate the applicability and effectiveness of the ITD algorithm. The main conclusion of this work is that the ITD algorithm is an efficient and reliable method to carry out the layout optimization of multi-material continuum structures.

ACKNOWLEDGEMENTS

This work was supported in part by the Departamento de Estructuras y Construcción at the Universidad Politécnica de Cartagena (Spain) and the Ministerio de Economía y Competitividad (Spain), via the research project DPI2011-26394. Its support is greatly appreciated.

REFERENCES

- Beaman JJ, Marcus HL, Bourell DL, Barlow JW, Crawford RH, McAlea KP. *Solid freeform fabrication: a new direction in manufacturing: with research and applications in thermal laser processing*. Kluwer Academic Publishers, 1997.
- Bhashyam S, Shin KH, Dutta D. An Integrated CAD System for the Design of Heterogeneous Objects. *Rapid Prototyping Journal*, **6**(2): 119-135, 2000.
- Blasques JP, Stolpe M. Multi-material topology optimization of laminated composite beam cross sections. *Composite Structures*, **94**: 3278-3289, 2012.
- Bourdin B, Chambolle A. Implementation of an adaptive finite element approximation of the Mumford-Shah functional. *Numer. Math.*, **85**(4): 609-646, 2000.
- Burger M, Stainko R. Phase-field relaxation of topology optimization with local stress constraints. *SIAM J. Control Optim.* **45**: 1447-1466, 2006.
- Cui C, Ohmori H, Sasaki M. Computational morphogenesis of 3D structures by extended ESO method. *Journal of IASS*, **44**(141): 51-61, 2003.
- Gao T, Zhang W, Duysinx P. Comparison of volume constraint and mass constraint in structural topology optimization with multiphase materials. *In proceedings of the 2nd International Conference on Engineering Optimization*, Lisbon, Portugal, 2010.
- Garcia MJ, Ruiz OE, Ruiz LM, Querin OM. Fixed grid finite element analysis for 3D linear elastic structures. *In proceedings of the Computational Mechanics. WCCM VI in conjunction with APCOM'04*, Beijing, China, 2004.
- García MJ, Steven GP. Fixed grid finite element analysis in structural design and optimization. *In proceedings of the Second ISSMO/AIAA Internet Conference on Approximations and Fast Reanalysis in Engineering Optimization*, 2000.
- Garcia MJ, Steven GP. Fixed grid finite elements in elasticity problems. *Engineering Computations*, **16** (2):145-164,1999.
- Garcia, Henao M, Ruiz OE. Fixed grid finite element analysis for 3D structural

- problems. *International Journal of Computational Methods*, **2**(4): 569-585, 2005.
- Hashin Z, Shtrikman S. A variational approach to the theory of the elastic behaviour of multiphase materials. *Journal of the Mechanics and Physics of Solids*, **11**(2): 127-140, 1963.
- Hinton A, Illingworth J. *Marching Triangles: Delaunay implicit surface triangulation*. Technical Report CVSSP 01, University of Surrey, Guildford, UK, 1997.
- Huang X, Xie YM. Bi-directional evolutionary topology optimization of continuum structures with one or multiple materials. *Comput. Mech.*, **43**: 393-401, 2009.
- Jadayil WA. Revision of the Recent Heterogeneous Solid Object Modeling Techniques. *Jordan Journal of Mechanical and Industrial Engineering*, **4**(6): 779-788, 2011.
- Jakubenas KJ, Sanchez JM, Marcus HL. Multiple material solid free-form fabrication by selective area laser deposition. *Materials and Design*, **19**(1-2): 11-18, 1998.
- Jung D, Gea HC. Design of an energy-absorbing structure using topology optimization with a multimaterial model. *Structural and Multidisciplinary Optimization*, **32**: 251-257, 2006.
- Koguchi A, Kikuchi N. A surface reconstruction algorithm for topology optimization. *Engineering with Computers*, **20**: 1-10, 2006.
- König O, Fadel GM. Applications of Genetic Algorithms in the design of Multi-Material Structures Manufactured in Rapid Prototyping. *In Proceedings of the Solid Freeform Fabrication Conference*, Austin TX, 1999.
- Luo Y, Kang Z, Yue Z. Maximal Stiffness Design of Two-Material Structures by Topology Optimization with Nonprobabilistic Reliability. *AIAA Journal*, **50**(9): 1993-2003, 2012.
- Maan FS, Querin OM, Barton DC. Extension of the fixed grid finite element method to eigenvalue problems. *Advances in Engineering Software*, **38**: 607-617, 2007.
- Nilsson S. Increasing strength of graphite/epoxy bolted joints by introducing and adhesively bonded metallic insert. *Journal of composite materials*, **2**: 642-650, 1989.
- Ramani A. A pseudo-sensitivity based discrete-variable approach to structural topology optimization with multiple materials. *Structural Multidisciplinary Optimization*. **41**: 913-934, 2010.
- Ramani A. Multi-material topology optimization with strength constraints. *Structural and Multidisciplinary Optimization*, **43**: 597-615, 2011.
- Rispler AR, Steven GP. Shape Optimisation of Metallic Inserts In Composite Bolted Joints. *In proceedings of the PICAST 2 – AAC 6*, Melbourne, 1995.
- Saxena A. On Multiple-Material Optimal Compliant Topologies: Discrete Variable Parameterization using Genetic Algorithm. *In proceedings of the SME2002 Design Engineering Technical Conferences and Computer and Information in*

Engineering Conference, Montreal, Canada, 2002.

- Sigmund O, Torquato S. Design of materials with extreme thermal expansion using a three-phase topology optimization method. *Journal of the Mechanics and Physics of Solids*, **45**(6): 1037-1067, 1997.
- Sigmund O. Design of multiphysics actuators using topology optimization part II: two material structures. *Computer Methods in Applied Mechanics and Engineering*, **190**: 6605-6627, 2001.
- Suresh S, Mortensen A. *Fundamentals of Functionally Graded Materials*, IDM Communications Ltd., 1988.
- Swan CC, Kosaka I. Voigt–Reuss topology optimization for structures with linear elastic material behaviors, *Int. J. Numer. Methods Engrg.*, **40**: 3033-3057, 1997.
- Takezawa A, Nishiwaki S, Kitamura M. Shape and topology optimization based on the phase field method and sensitivity analysis. *Journal of Computational Physics*, **229**(7): 2697-2718, 2010.
- Thomsen J. Topology optimization of structures composed of one or two materials. *Structural Optimization*, **5**: 108-115, 1992.
- Tsai A, Yezzi A, Willsky AS. Curve evolution implementation of the Mumford-Shah functional for image segmentation, denoising, interpolation, and magnification. *IEEE Trans. Image Process*, **10**(8): 1169-1186, 2001.
- Vese LA, Chan TF. A multiphase level set framework for image segmentation using the Mumford and Shah model. *Int. J. Comput. Vision*, **50**(3): 271-293, 2002.
- Victoria M, Martí P, Querin OM. Topology design of two-dimensional continuum structures using isolines. *Computer and Structures*, **87**: 101-109, 2009.
- Wang MY, Wang S. Bilateral filtering for structural topology optimization. *Int. J. Numer. Meth. Engrg.*, **63**: 1911-1938, 2005.
- Wang MY, Wang X. “Color” level sets: a multi-phase method for structural topology optimization with multiple materials. *Comput. Methods Appl. Mech. Engrg.*, **193**: 469-496, 2004.
- Wang MY, Zhou SW. Phase field: A variational method for structural topology optimization. *Comput. Model. Eng. Sci.*, **6**: 547-566, 2004.
- Woon SY, Tong L, Querin OM, Steven GP. Optimising topologies through a multi-GA System. *In proceedings of the Fifth World Congress of Structural and Multidisciplinary Optimization (WCSMO 5)*, Lido di Jesolo, 229-230, 2003.
- Yin L, Ananthasuresh GK. Topology optimization of compliant mechanisms with multiple materials using a peak function material interpolation scheme. *Structural and Multidisciplinary Optimization*, **23**: 49-62, 2001.
- Yulin M, Xiaoming W. A level set method for structural topology optimization and its applications. *Advances in Engineering Software*, **35**: 415-441, 2004.

- Zhao HK, Merriman B, Osher S, Wang L. Capturing the behaviour of bubbles and drops using the variational level set approach. *J. Comput. Phys*, **143**: 495-518, 1998.
- Zhou S, Wang MY. Multimaterial structural topology optimization with a generalized Cahn–Hilliard model of multiphase transition. *Structural and Multidisciplinary Optimization*, **33**: 89-111, 2007.
- Zhuang C, Xiong Z, Zhu X, Ding H. Von Mises Stress and Level Set Method based Structural Topology Optimization with Multi-phase Materials. *In proceedings of the 3rd Annual IEEE Conference on Automation Science and Engineering*, Scottsdale, AZ, 2007.